



## A novel way of detecting transient cavitation near a solid surface during megasonic cleaning using electrochemical impedance spectroscopy

M. Keswani\*, S. Raghavan, P. Deymier

Department of Materials Science and Engineering, University of Arizona, Tucson 85741, USA

### ARTICLE INFO

#### Article history:

Received 23 April 2012

Received in revised form 4 January 2013

Accepted 28 February 2013

Available online 14 March 2013

#### Keywords:

Megasonic cleaning

Transient cavitation

Acoustic streaming

Microelectrode

Electrochemical impedance spectroscopy

(EIS)

### ABSTRACT

Megasonic energy assisted wet cleaning is traditionally used for removal of particulate contaminants from wafer and mask surfaces in semiconductor industry. One of the major issues associated with megasonic cleaning is the damage caused to fragile features due to transient cavitation. Development of a method to monitor transient cavitation events in solutions irradiated with sound energy will allow chemical formulators to fine tune the cleaning chemistry and acoustic field parameters for maximum cleaning efficiency without any feature damage. In this work, a method based on electrochemical impedance spectroscopy (EIS) measurements on a microelectrode has been found to be effective in detection of transient cavity collapses in solutions subjected to  $\sim 1$  MHz sound field. Additionally, the technique also provides useful information about the diffusion boundary layer thicknesses in the presence and absence of megasonic field.

© 2013 Elsevier B.V. All rights reserved.

### 1. Introduction

The use of megasonic energy for wafer and mask cleaning has been of interest to semiconductor industry for many years [1,2]. Although, megasonic cleaning offers the advantage of high particle removal efficiency (PRE), it has limited application due to feature damage. Two principle mechanisms, namely, acoustic streaming and cavitation are known to predominantly occur in solutions irradiated with sound field [3–5]. It is generally believed that both streaming and cavitation are instrumental in particle removal whereas cavitation is the main cause of damage to fragile features [3,6].

Two types of cavitation exist in solutions subjected to acoustic energy, stable cavitation and transient cavitation [7]. Stable cavitation, acting as a secondary sound source and leading to microstreaming, entails oscillations of bubbles about an equilibrium size for many acoustic cycles. Transient cavitation is characterized by large bubble size variations and eventual bubble collapse, which can be quite violent. This violent collapse, accompanied by extremely high temperature and pressure conditions, often leads to the formation of shock waves or liquid jets, depending on the distance between the collapsing cavity and the solid surface [8,9]. Both shock waves and liquid jets are believed to be responsible for feature damage [10,11]. In order to reduce damage while maintaining high PRE, it is important to significantly lower transient cavitation in clean-

ing solutions without affecting streaming forces. This can be achieved by monitoring transient cavitation events in solutions using a suitable in situ technique and tuning the sound field and liquid parameters that will minimize collapse of transient cavities.

Ashokkumar et al., used a multi-bubble sonoluminescence based technique for detection of stable and transient cavitation in aqueous solutions containing up to 100 mM of propanol or acetone irradiated with acoustic frequencies in the range of 20–440 kHz [12]. Their study revealed that stable cavitation is existent at low sound frequency of 20–37 kHz and transient cavitation can occur at high sound frequency of 440 kHz. In another study, high time resolution microelectrode based electrochemical (chronoamperometry) technique was used to characterize transient cavitation in aqueous solutions exposed to ultrasonic field (20–100 kHz) [13]. Measurement of reduction current of ruthenium (III) hexamine at a microelectrode (10  $\mu\text{m}$ ) was used to monitor transient cavitation. The results of this study showed that increasing the acoustic pressure amplitude from 0.8 to 1.7 atm at  $\sim 40$  kHz of sound field increased the transient cavitation events from a few hundred to  $\sim 5000$  events per second.

Keswani et al., measured frequency of transient cavitation events in DI water saturated with different dissolved gases (Ar, N<sub>2</sub>, and CO<sub>2</sub>) as a function of megasonic ( $\sim 1$  MHz) power density using cyclic voltammetry measurements on a 25  $\mu\text{m}$  microelectrode [14]. It was reported that for Ar saturated solutions, the frequency of occurrence of transient cavitation (of certain collapse intensity) increased from  $\sim 5$  to 65 in 10 s with increase in power density from 0.4 to 2 W/cm<sup>2</sup>. Interestingly, when the experimental

\* Corresponding author.

E-mail address: [manishk@email.arizona.edu](mailto:manishk@email.arizona.edu) (M. Keswani).

solution contained saturated levels of  $N_2$  and  $CO_2$ , respectively, the transient cavitation events reduced to 35 and 5 (in 10 s) at  $2\text{ W/cm}^2$ . A novel method based on measurement of cavitation noise using a hydrophone was shown to be effective in characterizing stable and transient cavitation at  $\sim 1\text{ MHz}$  sound frequency generated in the power density range of  $0.012\text{--}0.4\text{ W/cm}^2$  [15]. In this technique, the peak levels of  $f/2$  and  $2f$  harmonics in the cavitation noise spectrum were shown to be good indicators of stable cavitation while the cavitation noise power was representative of transient cavitation.

In this paper, an alternative method for detection of transient cavitation at  $\sim 1\text{ MHz}$  of sound frequency is presented. The method is based on electrochemical impedance spectroscopy (EIS) measurements on a microelectrode in aqueous solutions containing an electroactive species such as potassium ferricyanide. Under reducing potentials for ferricyanide, when the applied AC frequency becomes comparable to the frequency of transient cavity collapses, the impedance values become unstable thereby revealing approximately the number of transient cavitation events occurring per unit time.

## 2. Materials and methods

Potassium ferricyanide ( $K_3Fe(CN)_6$ ), and potassium chloride (KCl), were of high purity ( $\geq 99.9\%$ ) and purchased from Sigma Aldrich. Platinum (Pt) wires ( $\geq 99\%$  purity) were obtained from Goodfellow. Electrochemical Impedance Spectroscopy (EIS) measurements were conducted in aqueous solutions at  $23 \pm 2^\circ\text{C}$  containing  $0.1\text{ M KCl}$  and  $0.05\text{ M K}_3\text{Fe(CN)}_6$  prepared using de-ionized (DI) water of resistivity  $18\text{ M}\Omega\text{-cm}$ . Prior to EIS measurements, the experimental solutions were de-oxygenated by bubbling with Ar gas ( $\geq 99\%$  purity) for 30 min followed by keeping an Ar blanket over the surface of the solution. Removal of oxygen from solutions is necessary to prevent any interference with ferricyanide reduction and was confirmed by measuring the dissolved oxygen content using an oxygen sensor (Rosemount Analytical model 499A DO).

The three electrode set up used for EIS experiments consisted of  $25\text{ }\mu\text{m}$  diameter disc as the working electrode (WE), and  $500\text{ }\mu\text{m}$  diameter Pt wires  $1\text{ cm}$  long as reference and counter electrodes (RE and CE). The three electrodes were enclosed in separate glass capillary tubes and arranged in a triangular manner. Pre-cleaning of Pt was done using reagent grade isopropyl alcohol (IPA) and flame heating to remove organic contaminants. Each of these steps was preceded by thorough DI water rinsing for 5 min and  $N_2$  drying.

For electrochemical measurements, the electrode set-up was placed in a ProSys<sup>®</sup> cylindrical tank (volume  $\sim 500\text{ ml}$ ) equipped with circular transducer (area  $22.2\text{ cm}^2$ ) that operates at  $\sim 1\text{ MHz}$  sound frequency. The working electrode was positioned close to the center of the transducer at  $\sim 2.0\text{ cm}$  above it. In cases of solutions exposed to megasonic energy, the transducer power density was set to  $2\text{ W/cm}^2$  and the mode of sound propagation was continuous, where the transducer was on for the entire measurement time. For cyclic voltammetry measurements, the potential was first scanned in the cathodic direction from open circuit potential (OCP) followed by reverse scan in the anodic direction and back to OCP at a rate of  $20\text{ mV/s}$ . In chronoamperometry experiments, the working electrode was biased at  $-0.1$ ,  $-0.4$  or  $-0.8\text{ V}$  potential and current was measured as a function of time at high sampling rate of 8 million samples per second. After about  $0.5\text{ s}$ , transducer was switched on for  $\sim 2\text{--}3\text{ s}$  at  $2\text{ W/cm}^2$ . The total time for measurement was about  $4\text{ s}$ . National Instrument Labview 9.0 was used for acquisition of the data, which was processed for graphical output using DIAdem 2010. Single sine EIS experiments were

performed at  $-0.2\text{ V}$  overpotential bias by sweeping the frequency from  $100\text{ kHz}$  to  $0.1\text{ Hz}$  using an AC rms voltage of  $\pm 10\text{ mV}$ . The sampling rate was fixed at 10 points per decade of frequency, where number of cycles at each AC frequency ranged between 2 and 20 with more cycles at higher frequency. Average of impedance values collected for several cycles at each frequency was used. Commercially available software, ZView (Version 2.9c), was used to fit the data to an equivalent circuit and calculate values of the circuit parameters.

## 3. Results and discussion

Cyclic voltammetry experiments were first performed on Pt ( $\sim 1\text{ cm}^2$ ) in deoxygenated  $2\text{ mM}$  potassium ferricyanide solution to determine the redox potential of the ferricyanide/ferricyanide couple. The results, in the form of a voltammogram, are shown in Fig. 1. As the potential is scanned from  $0\text{ V}$  to negative values, ferricyanide species reduce to ferrocyanide and a reduction (cathodic) peak is observed at  $-0.26\text{ V}$ . During the reverse (oxidation) cycle, when the ferrocyanide oxidizes to ferricyanide, an oxidation (anodic) peak occurs at  $-0.16\text{ V}$ . A peak separation of  $100\text{ mV}$ , which is larger than  $59\text{ mV}$  difference typically seen for a reversible redox reaction, indicates the behavior of the ferricyanide/ferricyanide couple to be quasi-reversible, as also reported in the literature [16]. The redox potential, calculated from the mean of peak cathodic potential and peak anodic potential, was found to be approximately  $-0.2\text{ V}$ .

Additionally, chronoamperometry experiments were also performed at various bias potentials of  $-0.1$ ,  $-0.4\text{ V}$  and  $-0.8\text{ V}$ . The microelectrode set up consisting of  $25\text{ }\mu\text{m}$  Pt working electrode was used. The solution contained  $50\text{ mM}$  potassium ferricyanide and  $100\text{ mM KCl}$ , which was deaerated by bubbling Ar gas. The sequence of events was as follows. The microelectrode was subjected to a suitable potential for a total period of  $4\text{ s}$ . During first  $0.5\text{ s}$  of applied potential, no megasonic field was applied. After this time, the solution was irradiated with  $\sim 1\text{ MHz}$  sound field at  $2\text{ W/cm}^2$  for  $2\text{--}3\text{ s}$ . Current was measured at 8 million samples per second for entire  $4\text{ s}$ . The results are shown in Fig. 2. As can be seen in the case of applied potential of  $-0.8\text{ V}$ , the baseline current in the absence of megasonic field is  $\sim 0.3\text{ }\mu\text{A}$ . This current increases to  $\sim 0.45\text{ }\mu\text{A}$  with current 'peaks' superimposed on it upon application of the megasonic field. The increase in baseline current has been attributed to enhanced diffusion due to acoustic streaming where as current 'peaks' are a result of transient cavitation. These have been discussed in detail elsewhere [14,17]. As the applied potential reduces to  $-0.4\text{ V}$ , there is no measurable difference in the baseline current or other features in the chronoamperometry

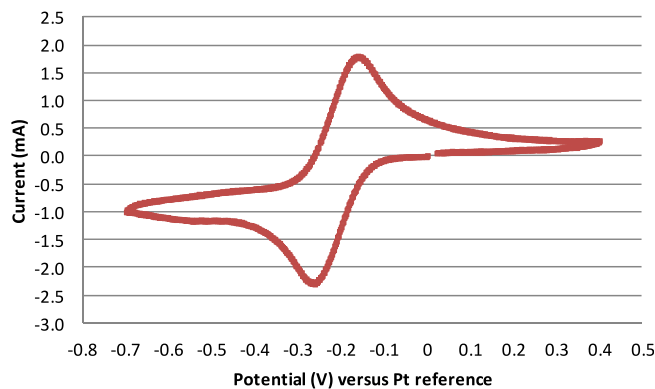
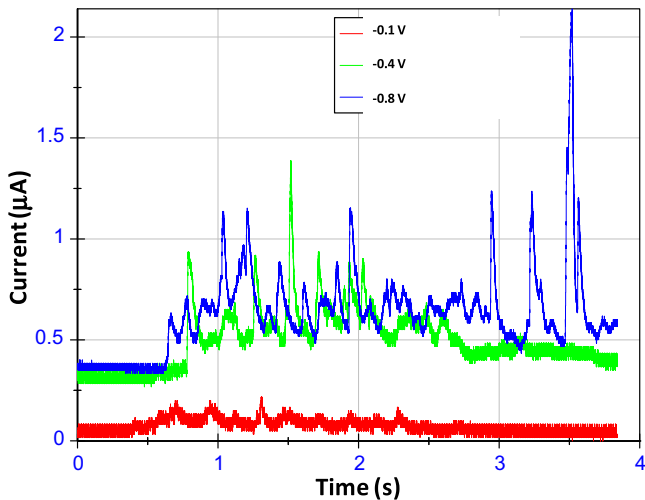


Fig. 1. Cyclic voltammetry on Pt ( $\sim 1\text{ cm}^2$ ) in deoxygenated  $2\text{ mM}$  potassium ferricyanide solution containing  $0.2\text{ M KCl}$  solution at a scan rate of  $20\text{ mV/s}$ . Pt used as the reference and counter electrode.



**Fig. 2.** Effect of applied potential on chronoamperometry current measured on 25  $\mu\text{m}$  Pt microelectrode in Ar saturated solution containing 50 mM potassium ferricyanide and 100 mM KCl. Current Sampling rate: 8 MS/s, Pt used as the reference and counter electrode. Data from  $\sim 0$ –0.5 s correspond to applied potential and no megasonic exposure, data from  $\sim 0.5$ –2.5 s (or 3.75 s) correspond to applied potential and megasonic exposure at 1 MHz and 2 W/cm<sup>2</sup>, data after  $\sim 2.5$  s for  $-0.1$  and  $-0.4$  V conditions correspond to applied potential and no megasonic exposure.

current. However, further reducing the applied potential to  $-0.1$  V apparently decreases the baseline current as well as the streaming current and magnitude of current ‘peaks’ due to transient cavitation. These results suggest that the required potential to completely reduce ferricyanide and create a diffusion limiting region near the electrode surface exists somewhere between  $-0.1$  and  $-0.4$  V. This further confirms the use of  $-0.2$  V as the appropriate potential for EIS studies as discussed below.

In the next step, EIS measurements at  $-0.2$  V (vs Pt reference) were performed on a 25  $\mu\text{m}$  Pt microelectrode in argon saturated 50 mM potassium ferricyanide solutions (containing 100 mM KCl) in the absence and presence of megasonic field. Nyquist and Bode plots obtained under silent conditions (no megasonic field) are shown in Fig. 3. A depressed semicircle is observed in the Nyquist plot indicating that the surface of the microelectrode is

not very smooth. A characteristic finite length Warburg diffusion response is also seen, which represents mass transfer limitation of ferricyanide species at the electrode surface due to its continuous reduction at  $-0.2$  V potential.

In the Bode plot of frequency versus phase angle, two characteristic curves with different time constants are observed. At higher frequency of  $10^5$  Hz, the phase angle is  $-50^\circ$  indicating contributions from both capacitive and reactive components to the current. The phase angle approaches a value of  $-10^\circ$  at lower frequency of 0.1 Hz suggesting dominance from reactive component.

In the presence of megasonic field at  $\sim 1$  MHz of sound frequency and 2 W/cm<sup>2</sup> of transducer power density, typical Nyquist and Bode plots obtained during EIS measurements are shown in Fig. 4. Comparing the data from Figs. 3 and 4, the impedance values measured in the presence of megasonic field are only slightly different compared to those measured in the absence of megasonic field for AC frequencies higher than 25 Hz. This indicates that megasonic field has no significant effect on impedance values when the AC frequency is above a critical value. This may be explained as follows. In megasonic field, fluid flow can occur either due to acoustic streaming or cavitation. It has been shown previously, that the transport of ferricyanide due to streaming forces is significantly smaller than that due to cavitation [14,17]. It is possible that due to weak flow of liquid from streaming and much lower frequency of occurrence of cavitation events compared to the frequency of AC cycle, the impedance values are not much affected by the application of megasonic field at higher AC frequencies.

At AC frequencies lower than 25 Hz, as can be seen from Fig. 4, the impedance values become unstable. This is likely due to frequency of occurrence of transient cavitation becoming comparable to the AC frequency ( $\leq 25$  Hz). As transient cavities collapse intermittently, they transport ferricyanide to the electrode surface which changes (reduces) the impedance values. Since the cavity collapse is not regular and may not occur at every AC cycle, the impedance values are not stable. Fluid movement in solution irradiated with megasonic field can occur due to acoustic streaming (Eckart, Rayleigh, Schlichting or microstreaming). However, since streaming flow is continuous (and does not occur in events), it can be expected to affect the impedance values at all AC frequencies and not just at frequencies below a critical value (25 Hz) as observed in the current data. Therefore, the possibility of fluid movement being the root

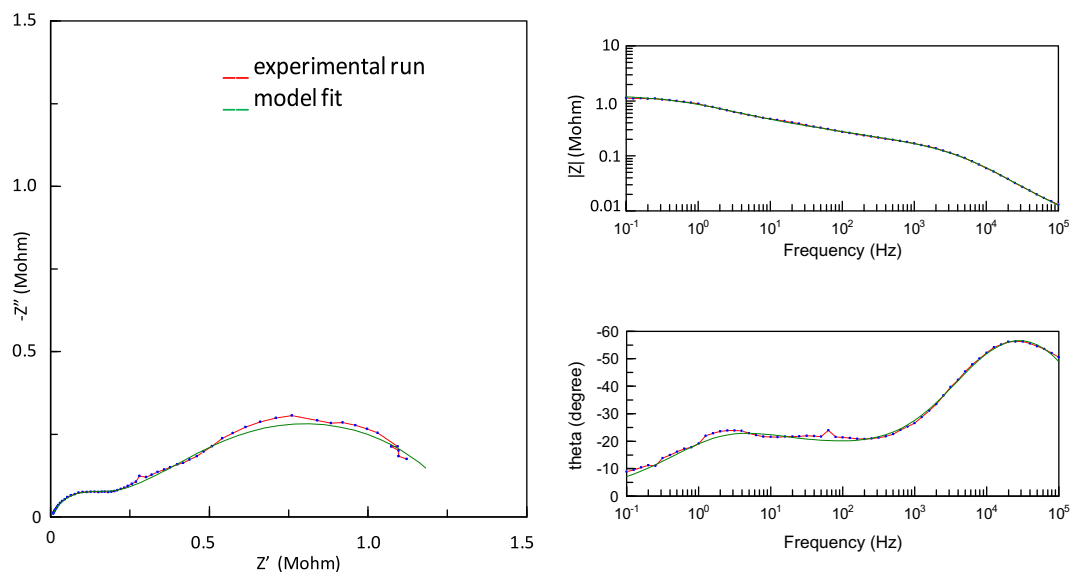


**Fig. 3.** Nyquist and Bode plots obtained from EIS measurements conducted on a 25  $\mu\text{m}$  Pt microelectrode held at  $-0.2$  V (vs Pt reference) in argon saturated solution (50 mM potassium ferricyanide and 0.1 M KCl) in the absence of megasonic field.

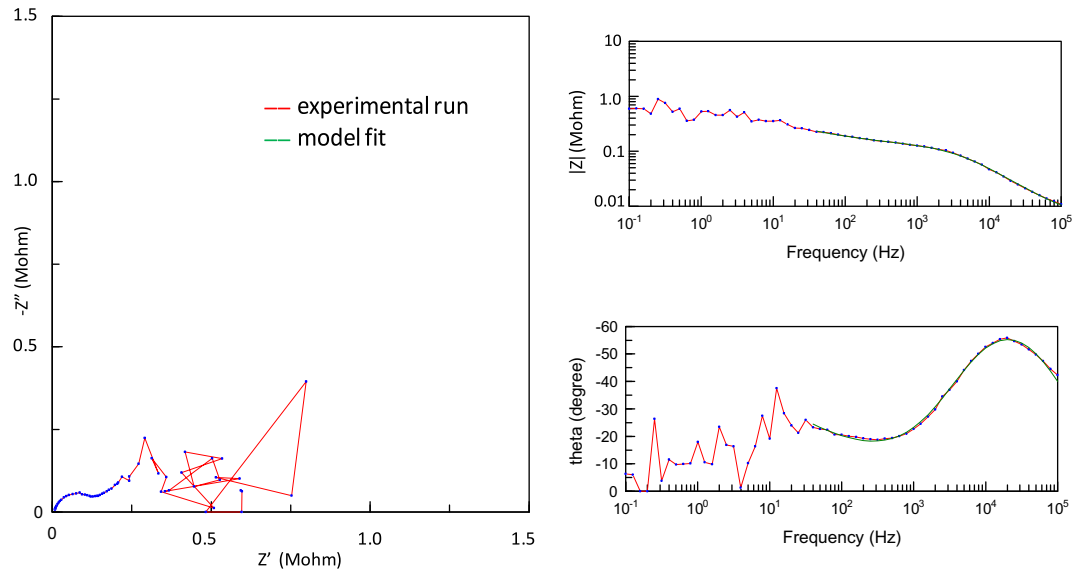


**Fig. 4.** Nyquist and Bode plots obtained from EIS measurements conducted on a 25  $\mu\text{m}$  Pt microelectrode held at  $-0.2$  V (vs Pt reference) in argon saturated solution (50 mM potassium ferricyanide and 0.1 M KCl) in the presence of megasonic field at  $\sim 1$  MHz of sound frequency and  $2$  W/cm $^2$  of transducer power density.

cause of the impedance fluctuations at AC frequencies  $\leq 25$  Hz can be ruled out. In order to ensure that this instability in impedance under megasonic conditions was not due to interference with electrical noise from the circuitry of the megasonic equipment, impedance measurements were performed in solutions without any megasonic exposure but with the megasonic equipment turned on in the close vicinity. No such instability in impedance was measured in this case. Further, for better visual comparison of the impedance results for megasonic and no megasonic conditions, the spectra (with a repeat measurement) for each of these cases are plotted in the same Fig. 5. Clearly, the differences in the spectra obtained in the presence and absence of megasonic irradiation of solutions are prominent at AC frequencies approximately lower than 25 Hz. The results of this study seems to correlate reasonably well with those published in literature [14], where it has been shown using cyclic voltammetry that transient cavitation events indeed occur at a frequency of 5–10 Hz in Ar saturated aqueous solution irradiated with sound field at 1 MHz and  $2$  W/cm $^2$ .

The impedance spectra (high frequency ( $>25$  Hz) or stable part of the spectrum for sound irradiated system and the entire data for silent conditions) were fitted to a typical modified Randles circuit with Warburg diffusion. A schematic of this model is shown in Fig. 6. In this model,  $R_s$  corresponds to the resistance of the aque-

ous solution,  $R_{ct}$  to the charge transfer resistance at the Pt/solution interface,  $CPE$  represents the constant phase element associated with the double layer capacitance at the Pt/solution interface, and  $W_s$  is the Warburg diffusion element of finite length.

The impedance of  $W_s$  (Eq. (1)) is defined as

$$Z_{W_s} = R \times \tan h[(j\omega\delta)^P] / (j\omega\delta)^P \quad (1)$$

where  $R$  corresponds to the Warburg element resistance related to the diffusion of the electroactive species (such as ferricyanide). The term  $(j\omega)$  is the product of  $j$ , an imaginary number equal to  $(-1)^{0.5}$ , and the angular frequency,  $\omega$ , which is  $2\pi$  times the linear AC frequency. The parameter  $\delta$  is related to the thickness,  $L$ , of the diffusion boundary layer and to the diffusion coefficient,  $D$ , through the relationship,  $\delta = (L^2/D)$ , and  $P$  is an exponent related to the slope of the linear part in the Nyquist plot.

The impedance of constant phase elements,  $CPE$ , is defined as

$$Z_{CPE} = 1/[T \times (j\omega)^P] \quad (2)$$

$CPE$  is essentially a distributed capacitor and its capacitance is given by  $CPE - T (\omega_m)^{P-1}$ , where  $\omega_m$  is the frequency at which the imaginary part of the impedance has a maximum and the exponent  $P$  is related to the surface roughness/inhomogeneity of the surface [18].  $CPE$  behaves like a pure capacitor when  $P = 1$ .

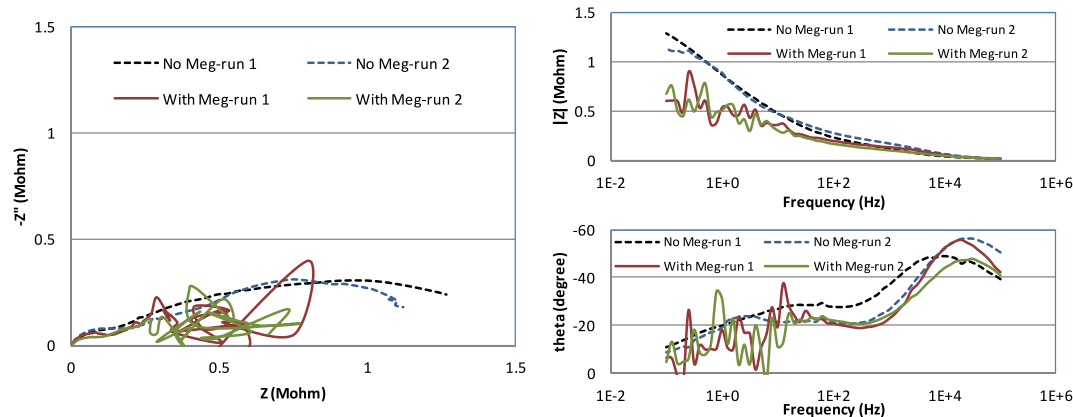


**Fig. 5.** Data from Figs. 3 and 4 along with repeat measurements for comparison purposes. Experimental Conditions stated in Figs. 3 and 4 for no megasonic and megasonic cases.

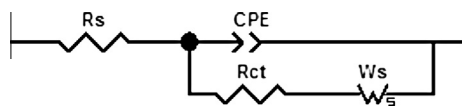


**Fig. 6.** Randle circuit model with mass transport limitations to fit impedance data obtained in this work.

**Table 1**

Parameters obtained from fitting the experimental data to a model based on modified Randles circuit with Warburg diffusion.

Parameters	–0.2 V (vs Pt) no meg	–0.2 V (vs Pt) meg 2 W/cm <sup>2</sup>
$R_s$ ( $\Omega$ )	$5100 \pm 10$	$5500 \pm 1000$
$CPE-T$ ( $\mu F \cdot s^{(P-1)}$ )	$3.5E-09 \pm 3.1E-09$	$3.2E-09 \pm 2.6E-09$
$CPE-P$	$0.8 \pm 0.05$	$0.81 \pm 0.07$
$R_{ct}$ ( $\Omega$ )	$0.97E05 \pm 0.4E05$	$1.1E05 \pm 0.2E05$
$W_s-R$ ( $\Omega$ )	$1.3E06 \pm 0.14E06$	$0.3E06 \pm 0.26E06$
$W_s-\delta$ (s)	$0.775 \pm 0.02$	$0.034 \pm 0.03$
$W_s-P$	$0.32 \pm 0.02$	$0.47 \pm 0.05$
$\chi^2$	$0.00095 \pm 0.00007$	$0.00045 \pm 0.0002$

The electrical parameters obtained from the fit of experimental data (shown in Fig. 5 for megasonic and no megasonic conditions) to the model are summarized in Table 1. A chi-square value lower than  $10^{-3}$  indicates good fitting between the experimental data and the model. The solution resistance is  $\sim 5100 \Omega$  and the double layer capacitance is  $80 \mu F/cm^2$ . A value of  $CPE-P$  ( $\sim 0.80$ ) less than 1.0 indicates some level of inhomogeneity on the platinum surface. The fitted values of the parameters,  $R$ ,  $T$  and  $P$  in the Warburg element, are represented by  $W-R$ ,  $W-\delta$  and  $W-P$ . A value of  $W-P$  lower than 0.5 for no megasonic case suggests that diffusion process is non uniform [19,20]. The diffusion layer thickness ( $L$ ) values in the absence and presence of megasonic field calculated from fitted  $W-\delta$  values and a diffusion coefficient ( $D = 0.7 \times 10^{-5} cm^2/s$ ) of ferricyanide ions [21,22] are 20 and  $7 \mu m$  respectively. The reduction in diffusion boundary layer thickness with application of megasonic field is expected due to mild streaming effect. These boundary layer thicknesses are consistent with the reported values in literature [14], which suggests that the choice of model is correct and also confirms the goodness of the fit. It is interesting to note that although diffusion boundary layer thickness is lower in the megasonic field,  $R_{ct}$  remains unaffected. This may be due to the fact that  $R_{ct}$  is dominated by the impedance values in the high frequency range where rate of diffusion will be the same in the presence and absence of megasonic field due to large thickness of boundary layer in both cases.

#### 4. Conclusions

Electrochemical Impedance Spectroscopy (EIS) measurements on a microelectrode in solutions irradiated with acoustic energy

at  $\sim 1$  MHz were found to be valuable in detecting transient cavitation events. At  $2.0 W/cm^2$  of transducer power density, the frequency of occurrence of transient cavitation collapses was determined to be of the order of 25 Hz. The diffusion layer thickness in the absence and presence of megasonic field was calculated to be 20 and  $7 \mu m$  respectively. The reduction in diffusion boundary layer thickness with application of megasonic field was attributed to weak flow of fluid due to acoustic streaming. In summary, impedance measurements using a microelectrode can be very effective in detecting the frequency of occurrence of transient cavitation events in different cleaning solutions used by semiconductor industry. The chemical formulators can use this technique to their benefit by tuning the sound field and cleaning chemistry variables for optimized cavitation to achieve maximum cleaning and minimum feature damage.

#### Acknowledgements

The authors acknowledge financial support from National Science Foundation (Award ID: 0925340). The authors would also like to thank Mark Beck of Product Systems, Inc. (ProSys) for donation and support of meg-bowl<sup>®</sup> equipment.

#### References

- [1] W. Kim, T. Kim, J. Choi, H. Kim, Appl. Phys. Lett. 94 (2009) 1–3. 081908.
- [2] A. Busnaina, J. Electrochem. Soc. 142 (1995) 2812–2817.
- [3] G. Gale, A. Busnaina, Part. Sci. Technol. 17 (1999) 229–238.
- [4] V. Kapila, P. Deymier, H. Shende, V. Pandit, S. Raghavan, F. Eschbach, Proc. SPIE – Int. Soc. Opt. Eng. 6283 (2006) 628324/1–628324/12.
- [5] P. Deymier, J. Vasseur, A. Khelif, D. Rouhani, L. Dobrzynski, S. Raghavan, J. Appl. Phys. 88 (2000) 6821–6835.
- [6] S. Kumari, M. Keswani, S. Singh, M. Beck, E. Liebscher, L. Toan, S. Raghavan, ECS Trans. 41 (5) (2011) 93–99.
- [7] M. Keswani, Ph.D Dissertation, The University of Arizona, Tucson, 2008.
- [8] C. Ohl, T. Kurz, R. Geisler, O. Lindau, W. Lauterborn, Philos. Trans. R. Soc. London, A 357 (1999) 269–294.
- [9] A. Philip, W. Lauterborn, J. Fluid Mech. 361 (1998) 75–116.
- [10] W. Schiffers, S. Shaw, D. Emmony, Ultrasonics 36 (1998) 559–563.
- [11] K. Suslick, G. Price, Annu. Rev. Mater. Sci. 29 (2009) 295–326.
- [12] M. Ashokkumar, J. Lee, Y. Iida, K. Yasui, T. Kozuka, T. Tuziuti, A. Towata, Phys. Chem. Chem. Phys. 11 (2009) 10118–10121.
- [13] P. Birkin, C. Delaplace, C. Bowen, J. Phys. Chem. B 102 (1998) 10885–10893.
- [14] M. Keswani, S. Raghavan, P. Deymier, Microelectron. Eng. 102 (2013) 91–97.
- [15] J. Frohly, S. Labouret, C. Bruneel, I. Looten-Baquet, R. Torguet, J. Acoust. Soc. Am. 108 (5) (2000) 2012–2020.
- [16] S. Petrovic, Chem. Educator 5 (5) (2000) 231–235.
- [17] M. Keswani, S. Raghavan, P. Deymier, Ultrason. Sonochem. 20 (2013) 603–609.
- [18] C. Hsu, F. Mansfeld, Corrosion 57 (9) (2001) 747–748.
- [19] J. Van Herle, A. McEvoy, J. Phys. Chem. Solids 55 (4) (1994) 339–347.
- [20] J. Molina, A. Rio, J. Bonastre, F. Cases, Eur. Polym. J. 45 (2009) 1302–1315.
- [21] S. Konopka, B. McDuffie, Anal. Chem. 42 (14) (1970) 1741–1746.
- [22] B. Pollet, J. Hihn, M. Doche, J. Lorimer, A. Mandroyan, T. Mason, J. Electrochem. Soc. 154 (10) (2007) E131–138.